ISSN 1674-1056
http://cpb.iphy.ac.cn
http://iopscience.iop.org/cpb
中国物理 B
Chinese Physics
中国物理 Chinese Physics B

Attosecond pulse trains driven by IR pulses spectrally broadened via supercontinuum generation in solid thin plates

Yu-Jiao Jiang(江昱佼)[1,2], Yue-Ying Liang(梁玥瑛)[2,3], Yi-Tan Gao(高亦谈)[2,3], Kun Zhao(赵昆)[2], Si-Yuan Xu(许思源)[1,2], Ji Wang(王佶)[2,4], Xin-Kui He(贺新奎)[2,5], Hao Teng(滕浩)[2], Jiang-Feng Zhu(朱江峰)[1], Yun-Lin Chen(陈云琳)[2,4], Zhi-Yi Wei(魏志义)[2,3,5]

Citation: Chin. Phys. B . 2020, 29(1): 013206 . **doi:** 10.1088/1674-1056/ab6315
Journal homepage: http://cpb.iphy.ac.cn; http://iopscience.iop.org/cpb

What follows is a list of articles you may be interested in

Observation of the optical $X^2\Sigma_g^+$-$A^2\Pi_u$ coupling in N_2^+ lasing induced by intense laser field

Siqi Wang(王思琪), Yao Fu(付尧), Danwen Yao(姚丹雯), Shanming Chen(陈善铭), Wei Zhang(张维), Helong Li(李贺龙), Huailiang Xu(徐淮良)

Chin. Phys. B . 2019, 28(12): 123301 . **doi:** 10.1088/1674-1056/ab54b1

Attosecond transient absorption spectroscopy: Comparative study based on three-level modeling

Zeng-Qiang Yang(杨增强), Di-Fa Ye(叶地发), Li-Bin Fu(傅立斌)

Chin. Phys. B . 2018, 27(1): 013301 . **doi:** 10.1088/1674-1056/27/1/013301

Semiclassical investigation of Coulomb focusing effects in atomic above-threshold ionization with elliptically polarized laser fields

Chuan-Liang Wang(王传亮), Li-Xin Xia(夏立新), Hong-Bin Yao(姚洪斌), Wen-Liang Li(李文亮)

Chin. Phys. B . 2017, 26(4): 043201 . **doi:** 10.1088/1674-1056/26/4/043201

Photoionization microscopy of Rydberg hydrogen atom in a non-uniform electrical field

Shao-Hao Cheng(程绍昊), De-Hua Wang(王德华), Zhao-Hang Chen(陈召杭), Qiang Chen(陈强)

Chin. Phys. B . 2016, 25(6): 063201 . **doi:** 10.1088/1674-1056/25/6/063201

Relativistic *R*-matrix studies of photoionization processes of Ar^{5+}

Li Chuan-Ying, Han Xiao-Ying, Wang Jian-Guo, Qu Yi-Zhi

Chin. Phys. B . 2013, 22(12): 123201 . **doi:** 10.1088/1674-1056/22/12/123201

RAPID COMMUNICATION

Attosecond pulse trains driven by IR pulses spectrally broadened via supercontinuum generation in solid thin plates*

Yu-Jiao Jiang(江昱佼)[1,2], Yue-Ying Liang(梁玥瑛)[2,3], Yi-Tan Gao(高亦谈)[2,3], Kun Zhao(赵昆)[2,†], Si-Yuan Xu(许思源)[1,2], Ji Wang(王佶)[2,4], Xin-Kui He(贺新奎)[2,5], Hao Teng(滕浩)[2], Jiang-Feng Zhu(朱江峰)[1], Yun-Lin Chen(陈云琳)[4], and Zhi-Yi Wei(魏志义)[2,3,5,‡]

[1] *School of Physics and Optoelectronic Engineering, Xidian University, Xi'an* 710071, *China*
[2] *Beijing National Laboratory for Condensed Matter Physics, Institute of Physics, Chinese Academy of Sciences, Beijing* 100190, *China*
[3] *University of Chinese Academy of Sciences, Beijing* 100049, *China*
[4] *Institute of Applied Micro-Nano Materials, School of Science, Beijing Jiaotong University, Beijing* 100044, *China*
[5] *Songshan Lake Material Laboratory, Dongguan* 523808, *China*

(Received 15 November 2019; revised manuscript received 14 December 2019; accepted manuscript online 18 December 2019)

We utilized a set of fused silica thin plates to broaden the spectrum of 1 kHz, 30 fs Ti:sapphire amplified laser pulses to an octave. Following the compression by chirped mirror pairs, the generated few-cycle pulses were focused onto an argon filled gas cell. We detected high order harmonics corresponding to a train of 209 as pulses, characterized by the reconstruction of attosecond beating by interference of two-photon transition (RABITT) technique. Compared with the conventional attosecond pulse trains, the broad harmonics in such pulse trains cover more energy range, so it is more efficient in studying some typical cases, such as resonances, with frequency resolved RABITT. As the solid thin plates can support high power supercontinuum generation, it is feasible to tailor the spectrum to have different central wavelength and spectral width, which will make the RABITT source work in different applications.

Keywords: supercontinuum generation, high order harmonic generation, reconstruction of attosecond beating by interference of two-photon transition (RABITT), attosecond pulse trains

PACS: 32.80.Fb, 33.20.Xx, 42.65.Ky, 42.65.Re **DOI:** 10.1088/1674-1056/ab6315

1. Introduction

Today, pump–probe scheme using ultrafast laser pulses acts as a crucial method in studying microscopic dynamics. After femtosecond-pump/femtosecond-probe experiments revealed the real-time evolution of chemical reactions,[1,2] lots of dynamics that take place within picoseconds were studied. In 2001, attosecond pulse trains (APT)[3] as well as isolated attosecond pulses (IAP)[4] were corroborated, and the pump–probe experiment soon made its debut in attosecond physics,[5] showing that movements of electrons can be captured. APT as well as IAP shed light on electron dynamics in different materials,[6,7] through analyzing the electron wave packet[8] which was angular resolved,[9] or the transient absorption spectrum.[10]

Since IAP covers a continuous spectrum and is definite in time, it enables us to reveal dynamics lasting from subfemtosecond to tens of femtoseconds. A popular method to record the ultrafast movement in a target is cross-correlation of an IAP and a femtosecond infrared (IR) pulse, which may be explained by the strong field approximation (SFA).[11] However, the strong femtosecond streaking field in such cross-correlation experiments may deform the signals to be measured,[12] and the background noise may also smear the finest structures. On the contrary, the reconstruction of attosecond beating by interference of two-photon transition (RABITT) technique by means of measuring the group delay of the electron wave packet operates under much lower IR intensity, and the phases of the sidebands are easier to be recognized and extracted.[13]

Phases obtained in a standard RABITT experiment represent an average over the energy components in each sideband. Recently, spectrally resolved RABITT (rainbow RABITT) has been developed to access phases at each photoelectron energy in the sidebands,[14,15] which is better in studying atomic or molecular resonance. Because practical issues often lead to broadening of the electronic transition line width (see supplementary materials of Ref. [14]), using rainbow RABITT to study resonance needs to cover a much broader energy range than the resonance line width itself. However, the discrete high order harmonics have limited spectral widths, which sometimes cannot cover the entire energy range of the transitions

*Project supported by the National Key R&D Program of China (Grant No. 2017YFB0405202), the Major Program of the National Natural Science Foundation of China (Grant No. 61690221), the Key Program of the National Natural Science Foundation of China (Grant No. 11434016), and the National Natural Science Foundation of China (Grant Nos. 11574384, 11674386, and 11774277).

†Corresponding author. E-mail: zhaokun@iphy.ac.cn
‡Corresponding author. E-mail: zywei@iphy.ac.cn

under study. To overcome this drawback, tunable IR pulses were employed to generate tunable APT to scan over consecutive spectral ranges or at least the range interested to study resonance transitions.[15,16] However, the tunability is often limited for most laser apparatus. Broad single order harmonics have a better opportunity to reach the energy level to be studied, but it may cause a spectral overlap between the harmonics and sidebands, and broadband femtosecond driving pulses will also deteriorate the electron spectrum resolution of the sidebands.[15] To this end, we search for a RABITT source that can cover the energy level to be studied, with appropriate energy and bandwidth. Few-cycle femtosecond pulses instead of narrow band long pulses could be a versatile source to drive high-order harmonic generation (HHG). On the one hand, such broadband pulses may produce broad harmonics to study a broad energy range. On the other hand, the broad spectrum of the driving pulses allows using optical filters to tailor and control its spectrum and pulse width then to control the energy and bandwidth of the HHG. To produce high-power, few-cycle pulses, the hollow core fiber (HCF) is a proven choice.[17–19] Here an alternative with a set of solid thin plates (STPs) shows higher efficiency, less sensitivity for beam pointing, and higher coherence.

2. Experimental setup

Figure 1 is a sketch of supercontinuum generation using a set of fused silica thin plates. 1 kHz, 0.8 mJ, 30 fs pulses centered at 790 nm from a Ti:sapphire chirped pulse amplification (CPA) laser system are loosely focused onto 7×100-μm-thick fused silica plates with a focusing lens ($f = 2000$ mm). We choose fused silica because it has large bandwidth, high transmission, high purity, and good uniformity. The spectrum is stretched to span an octave due to self-phase modulation (SPM) and self-steepening, and it can be compressed to 5.4 fs with 0.58 mJ output energy of the central part of the Bessel beam after chirped mirror pairs and fused silica wedges.[20] For HCF differentially filled with neon with the same input pulse energy, the output energy is about 0.4 mJ with sub 5 fs pulse width.

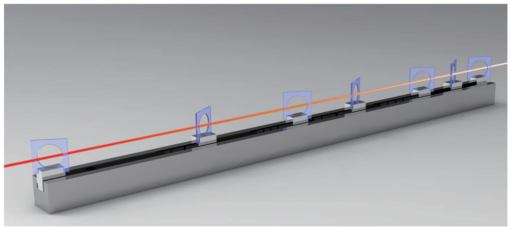

Fig. 1. Supercontinuum generation using STPs.

We use the propagation equation to simulate the spectral broadening after 7 thin fused silica plates.[21] The simulated spectrum after the thin plates is shown in Fig. 2. Except the sudden decrease around 650 nm, our measured spectrum agrees with the simulation.

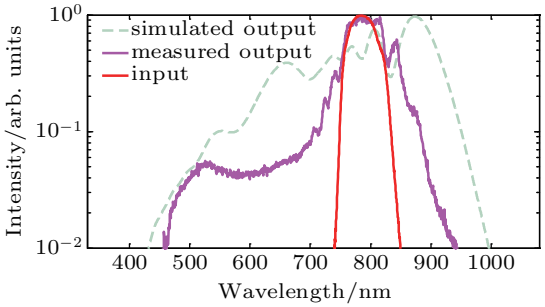

Fig. 2. Spectra before/after the fused silica thin plates. Red solid line is the CPA laser spectrum, magenta solid line is the measured spectrum after the thin plates, and green dotted line is the simulated spectrum after the thin plates.

Coherence of the driving field strongly affects the coherence length and efficiency of HHG.[22] The driving field also serves as the probe pulse in RABITT or streaking experiments, so it is meaningful to use a high coherence driving field. The coherence of the driving field determines the best fringe contrast in the spectral interference measurement of the carrier envelop phase (CEP), as well as in the root mean square (RMS) of the CEP after phase locking,[23] which is an important parameter of the few cycle laser field. As a nonlinear optical material, solid is more stable, when not ionized, than the noble gas in HCF. The thin structure is beneficial for releasing heat, which improves the stability of the output pulses, and consequently, the coherence of the output pulses. To evaluate the coherence of the output pulse, we apply an f–$2f$ interferometer[24] for CEP locking after STPs and HCF under the same input pulse condition. We find that the spectral interference modulation after STPs is indeed deeper than that after HCF. The measured RMS of CEP is 346 mrad after STPs and 540 mrad after HCF under 3 ms integration time, compared with 34 mrad and 107 mrad simulation results, respectively. The best CEP locking result we have got experimentally after STPs is 227 mrad RMS under 3 ms integration time for 20 min.[25] These results are consistent with each other, indicating that the pulses after STPs are more coherent than those after HCF.

We focus this pulse by a low group delay dispersion (GDD) silver concave mirror with focal length of 400 mm, to an Ar filled gas cell. The beam line is illustrated in Fig. 3. High order harmonics are generated in the gas cell at the center of the IR beam, then they co-propagate with the IR pulse with a smaller radius and divergence.[26] A 200 nm-thick Al filter blocks the residual IR and lets part of the high order harmonics transmit while compensating the attochirp. The high order harmonic spectrum is detected by an extreme-ultraviolet (XUV) charge-coupled device (CCD) at the end of the beam line. The Al filter can be switched to a smaller one mounted

at the center of a 7.5 μm thick tensioned annular Kapton pellicle. When this filter is in the beam path of the co-propagating pulses, the Al filter blocks the residual IR at the center, and the annular pellicle blocks the high order harmonics. By using this filter, the XUV and IR beams are separated spatially. The separated round XUV pulse and annular IR pulse are focused by the inner and outer parts of a Mo–Si multilayer mirror set, respectively. This mirror set contains an inner round part and an outer annular part, which is cut from a Mo–Si multilayer coated concave mirror with a focal length of 125 mm. The inner part is mounted on a piezo transducer (PZT) in close loop mode to adjust the delay between the XUV and IR pulses. A motorized iris is applied before the filter to adjust the IR pulse intensity. An Ar gas jet is mounted near the focal spot of the Mo–Si mirror. An electron time-of-flight (TOF) spectrometer records the photo-electron kinetic energy when the Ar atoms are ionized by the high-order harmonics with the existence of the IR pulses.[19]

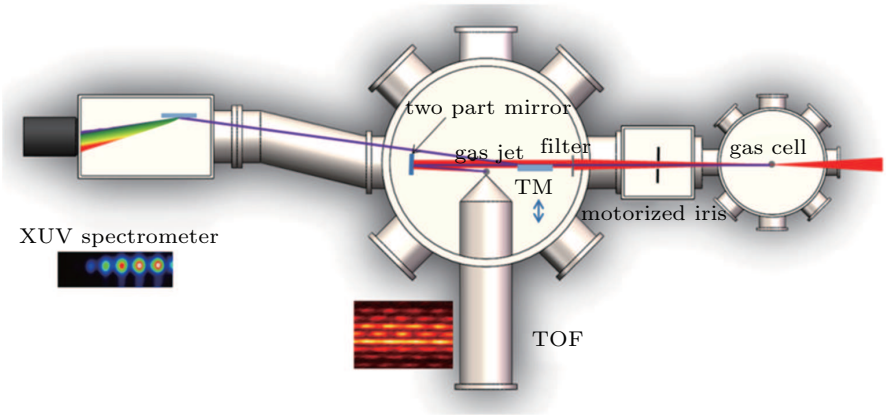

Fig. 3. Attosecond streaking/RABITT beam line. TM: toroidal mirror (insert into the beam path to inspect high order harmonics on the XUV spectrometer). TOF: time of flight.

When we block the IR pulses, a photoelectron energy spectrum is produced via Ar ionization by the XUV pulses only. As illustrated in Fig. 4, the blue line is the XUV photon spectrum shifted from the measured photoelectron spectrum, and the pink one is the XUV spectrum simulated by SFA. The reflectivity of the Mo–Si multilayer mirror has minima around 26.7 eV and 36.1 eV. A single harmonic in the measured result covers more than 2.8 eV (full width at half maximum (FWHM), ∼1.6 eV). While the odd harmonics are separated by 3.1 eV, this is not ideal for RABITT experiments, since the sidebands will mingle with the harmonics.

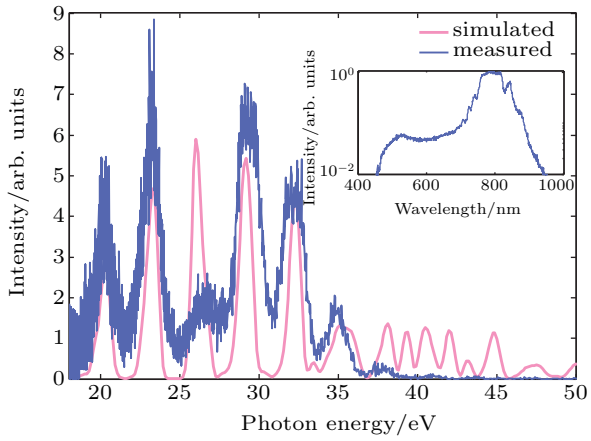

Fig. 4. High order harmonic spectrum derived from photoelectron spectrum of Ar ionization and the corresponding simulation result. The high order harmonics are generated by few-cycle IR pulses from STPs. The inset shows the spectrum of the IR pulse produced by spectral broadening in STPs.

To obtain a good RABITT trace, we reduce the input pulse energy for the fused silica thin plates to 0.53 mJ to get a less broad spectrum. Based on the autocorrelation signal of the photoelectrons from above-threshold ionization initiated by the IR pulses, the pulse width is estimated to be about 10 fs. The RABITT signal recorded is depicted in Fig. 5. This graph

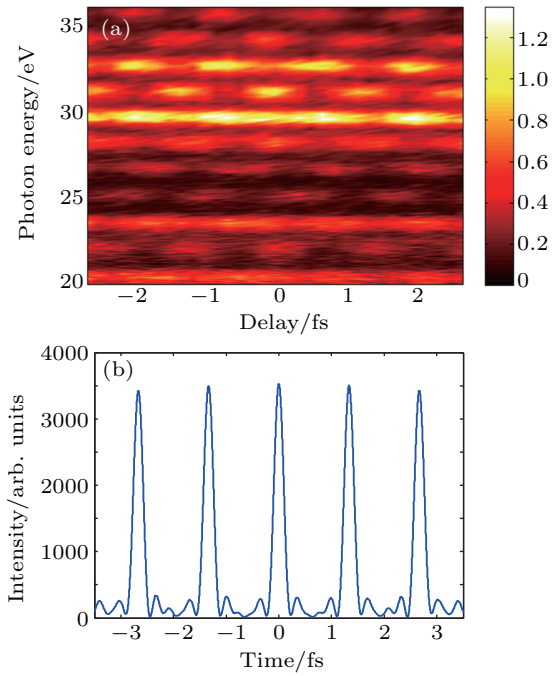

Fig. 5. (a) RABITT trace obtained with respect to time delay between IR pulses and attosecond pulse trains (the time zero is not absolute). The vertical coordinate stands for high order harmonic photon energy. (b) Reconstructed attosecond pulse trains.

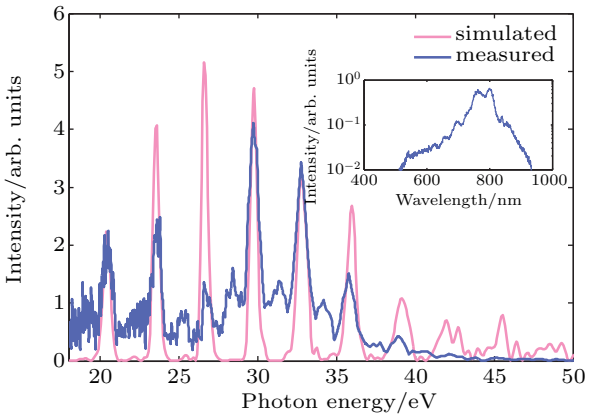

Fig. 6. Measured high order harmonic spectrum with weak sidebands (blue) compared with the simulated result (red). Inset: supercontinuum spectrum which drives the HHG.

consists of 33 electron spectra at different delays of the pump and probe pulses with a step of 0.05 μm, and each spectrum is acquired in 200 s. This indicates that our high harmonic source is stable within 110 min. Each harmonic covers 0.9 eV, which is broad enough to cover a large energy range, such as a Fano resonance, but not mixed with the sidebands. The reconstructed attosecond pulse trains are shown in Fig. 5. The FWHM of each pulse is 209 as.

We also compare the experimental HHG spectrum with the simulated one driven by 8 fs, 790 nm central wavelength pulses, as shown in Fig. 6. Good agreement is observed.

3. Simulation and prospect

As the STPs support high output energy, it is possible to use band pass filters to remove part of the IR spectrum and make the few-cycle IR pulses versatile for different applications. Figure 7 shows the simulated high order harmonic

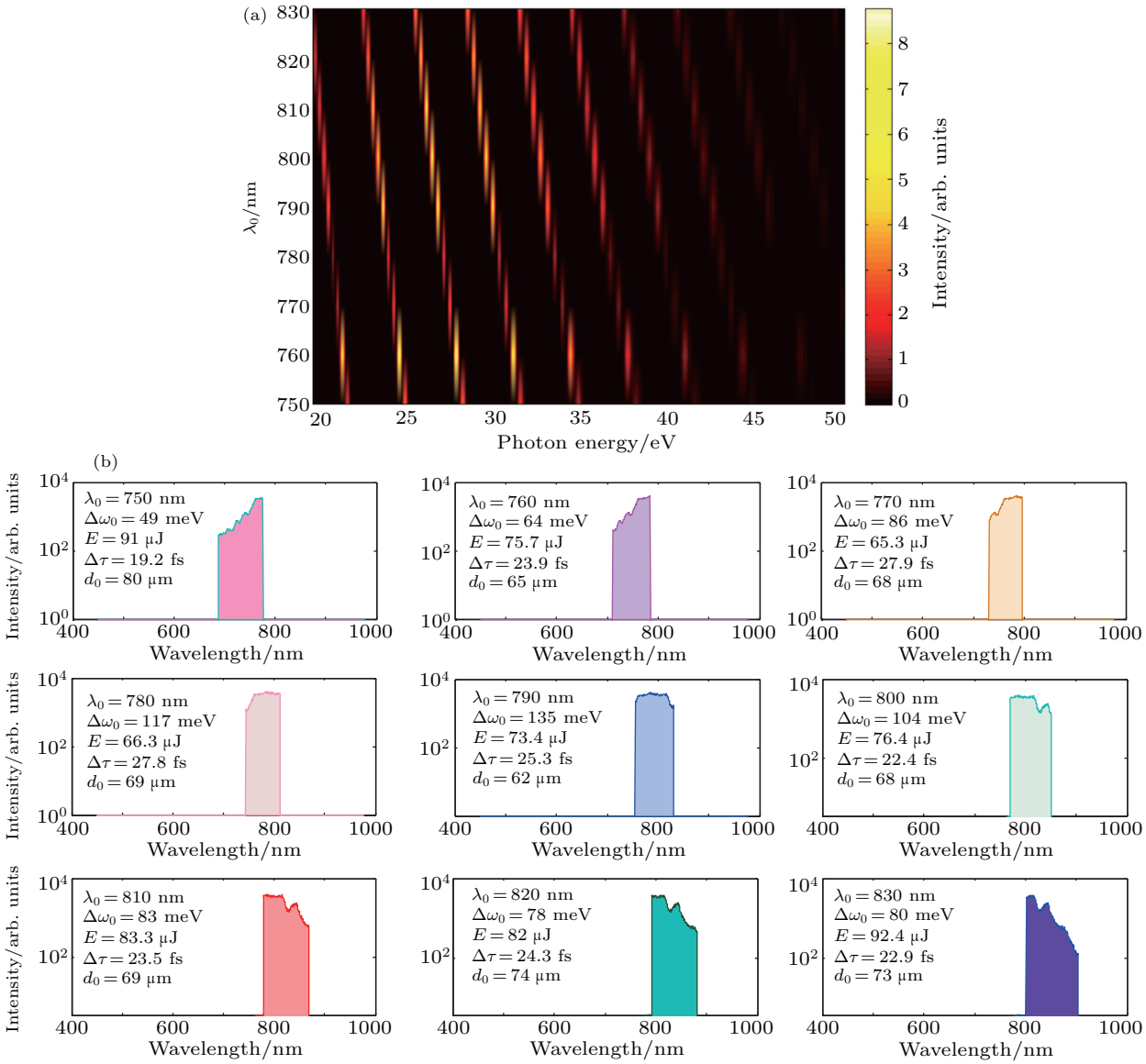

Fig. 7. Calculated high order harmonic spectra (a) driven by filtered IR spectra (b). λ_0: central wavelength of the filtered pulse, $\Delta\omega_0$: band width of the filtered pulse, E: pulse energy after the band pass filter, $\Delta\tau$: transform limited FWHM of the filtered pulse, d_0: diameter of the beam waist for HHG simulation.

spectra using filtered driving IR spectra. We list the central wavelength and bandwidth of the HHG driving pulse after the spectral filters using the high input power mode of the STPs setup, as shown in Fig. 7(b), then we simulate the corresponding high order harmonic spectra,[27,28] as shown in Fig. 7(a). By changing the spectral filter, one can make the Ti:sapphire CPA pulse quasi tunable to cover more wavelength range. For example, $3s3p^6np$ argon Fano resonance energy levels are 26.606 eV ($n = 4$), 27.993 eV ($n = 5$), 28.506 eV ($n = 6$), and 28.757 eV ($n = 7$),[29] by using different filters after STPs, all of them can be studied. For another example, when studying ionization delays from close bonding energy level in molecules with RABITT method, the sidebands of neighboring high order harmonics of electrons with different bonding energy may be very close to each other.[30] Although narrow band high order harmonics will make it easier to find out the specific sideband, the energy sampling distance is the same as that of the odd high order harmonics. With the filters applied after STPs, the energy sampling distance can be significantly shortened while the sidebands can be distinguished. The dispersion introduced by the filters may be compensated by chirped mirror pairs. We also list the diameters of the driving beam waist to calculate the HHG. The single harmonic covers typically 200 meV to maintain the IR width under 135 meV for high resolution application, one can change the band pass filter to select broader spectrum of IR pulse for broader harmonic width.

In certain applications of attosecond optics, a higher repetition rate is favorable. For this purpose, the high repetition rate Yb: KGW chirped-pulse amplifier is a good choice,[31] and STPs also works well with Yb:KGW CPA.[32,33]

4. Conclusion

We use STPs to broaden the spectrum of 0.8 mJ, 1 kHz Ti:sapphire CPA pulses to an octave. After dispersion compensation, 5.4 fs output pulse with 0.58 mJ energy of the central part of the Bessel beam is measured using TG-FROG.[34] The output pulse shows better efficiency and coherence than that compressed by HCF. Then the pulses are used for HHG in Ar. The generated high order harmonics are focused on a second Ar gas jet, and photoelectron is recorded using TOF. The harmonics are separated by 3.1 eV, and the full width of a single harmonic is more than 2.8 eV which is too broad for RABITT. When we decrease the input pulse onto the STPs to 0.53 mJ, SPM is less significant, thus the output spectrum is narrower. We apply this pulse to HHG and perform the RABITT experiment. The attosecond pulse trains are stable and the FWHM of each pulse is around 209 as. Besides broadband RABITT, we also simulate the high order harmonics using 5.4 fs, 0.58 mJ pulses after different band pass filters. By changing the filters, high order harmonics cover a consecutive energy range, indicating one can make the Ti:sapphire CPA pulses quasi tunable for different applications based on RABITT scheme. As a general supercontinuum generation method with high efficiency and high coherence for pump pulses with different wavelengths, we suggest to use STPs in combination with different pump lasers for RABITT sources and applications.

References

[1] Rosker M J, Dantus M and Zewail A H 1988 *J. Chem. Phys.* **89** 6113
[2] Zewail A H 2000 *J. Phys. Chem. A* **104** 5660
[3] Paul P M, Toma E S, Breger P, Mullot G, Augé F, Balcou P, Muller H G and Agostini P 2001 *Science* **292** 1689
[4] Hentschel M, Kienberger R, Spielmann C, Reider G A, Milosevic N, Brabec T, Corkum P, Heinzmann U, Drescher M and Krausz F 2001 *Nature* **414** 509
[5] Drescher M, Hentschel M, Kienberger R, Uiberacker M, Yakovlev V, Scrinzi A, Westerwalbesloh T, Kleineberg U, Heinzmann U and Krausz F 2002 *Nature* **419** 803
[6] Locher R, Castiglioni L, Lucchini M, Greif M, Gallmann L, Osterwalder J, Hengsberger M and Keller U 2015 *Optica* **2** 405
[7] Cavalieri A L, Müller N, Uphues T, Yakovlev V S, Baltuška A, Horvath B, Schmidt B, Blümel L, Holzwarth R, Hendel S, Drescher M, Kleineberg U, Echenique P M, Kienberger R, Krausz F and Heinzmann U 2007 *Nature* **449** 1029
[8] Ossiander M, Siegrist F, Shirvanyan V, Pazourek R, Sommer A, Latka T, Guggenmos A, Nagele S, Feist J, Burgdörfer J, Kienberger R and Schultze M 2017 *Nat. Phys.* **13** 280
[9] Cirelli C, Marante C, Heuser S, Petersson C L M, Galán Á J, Argenti L, Zhong S, Busto D, Isinger M, Nandi S, Maclot S, Rading L, Johnsson P, Gisselbrecht M, Lucchini M, Gallmann L, Dahlström J M, Lindroth E, Huillier A, Martín F and Keller U 2018 *Nat. Commun.* **9** 955
[10] Wang H, Chini M, Chen S, Zhang C, He F, Cheng Y, Wu Y, Thumm U and Chang Z 2010 *Phys. Rev. Lett.* **105** 143002
[11] Kitzler M, Milosevic N, Scrinzi A, Krausz F and Brabec T 2002 *Phys. Rev. Lett.* **88** 173904
[12] Cattaneo L, Vos J, Lucchini M, Gallmann L, Cirelli C and Keller U 2016 *Opt. Express* **24** 29060
[13] Klünder K, Dahlström M, Gisselbrecht M, Fordell T, Swoboda M, Guenot D, Johnsson P, Caillat J, Mauritsson J, Maquet A, Taieb R and Huillier A 2011 *Phys. Rev. Lett.* **106** 143002
[14] Gruson V, Barreau L, Jiménez-Galan Á Risoud F, Caillat J, Maquet A, Carré B, Lepetit F, Hergott J F, Ruchon T, Argenti L, Taïeb R, Martín F and Salières P 2016 *Science* **354** 734
[15] Busto D, Barreau L, Isinger M, Turconi M, Alexandridi C, Harth A, Zhong S, Squibb R J, Kroon D, Plogmaker S, Miranda M, Jiménez-Galán Á Argenti L, Arnold C L, Feifel R, Martín F, Gisselbrecht M, Huillier A and Salières P 2018 *J. Phys. B: At. Mol. Opt. Phys.* **51** 044002
[16] Kotur M, Guénot D, Jiménez-Galán Á Kroon D, Larsen E W, Louisy M, Bengtsson S, Miranda M, Mauritsson J, Arnold C L, Canton S E, Gisselbrecht M, Carette T, Dahlström J M, Lindroth E, Maquet A, Argenti L, Martín F and Huillier A 2016 *Nat. Commun.* **7** 10566
[17] Nisoli M, Silvestri S D and Svelto O 1996 *Appl. Phys. Lett.* **68** 2793
[18] Nisoli M, Silvestri S D, Svelto O, Szipöcs R, Ferencz K, Spielmann C, Sartania S and Krausz F 1997 *Opt. Lett.* **22** 522
[19] Zhan M J, Ye P, Teng H, He X K, Zhang W, Zhong S Y, Wang L F, Yun C X and Wei Z Y 2013 *Chin. Phys. Lett.* **30** 093201
[20] He P, Liu Y, Zhao K, Teng H, He X, Huang P, Huang H, Zhong S, Jiang Y, Fang S, Hou X and Wei Z 2017 *Opt. Lett.* **42** 474
[21] Bergé L, Skupin S, Nuter R, Kasparian J and Wolf J P 2007 *Rep. Prog. Phys.* **70** 1633

[22] Huillier A, Schafert K J and Kulande K C 1991 *J. Phys. B: At. Mol. Opt. Phys.* **24** 3315

[23] Raabe N, Feng T, Witting T, Demircan A, Brée C and Steinmeyer G 2017 *Phys. Rev. Lett.* **119** 123901

[24] Jones D J, Diddams S A, Ranka J K, Stentz A, Windeler R S, Hall J L and Cundiff S T 2000 *Science* **288** 635

[25] Jiang Y, Gao Y, Huang P, Zhao K, Xu S, Zhu J, Fang S, Teng H, Hou X and Wei Z 2019 *Acta Phys. Sin.* **68** 214204 (in Chinese)

[26] Chang Z 2011 *Fundamentals of Attosecond Optics* (1st Edn.) (Boca Raton: Taylor and Francis Group) p. 39

[27] Lewenstein M, Balcou P, Ivanov M Y, Huillier A and Corkum P B 1994 *Phys. Rev. A* **49** 2117

[28] Priori E, Cerullo G, Nisoli M, Stagira S, Silvestri S D, Villoresi P, Poletto L, Ceccherini P, Altucci C, Bruzzese R and Lisio C 2000 *Phys. Rev. A* **61** 063801

[29] Sorensen S L, Aberg T, Tulkki J, Rachlew-kallen E, Sundestrom G and Kirm M 1994 *Phys. Rev. A* **50** 1218

[30] Huppert M, Jordan I, Baykusheva D, Conta A and Wörner H J 2016 *Phys. Rev. Lett.* **117** 093001

[31] Beetar J E, Gholam-Mirzaei S and Chini M 2018 *Appl. Phys. Lett.* **112** 051102

[32] Ishii N, Xia P, Kanai T and Itatani J 2019 *Opt. Express* **27** 11447

[33] Lu C, Wu W, Kuo S, Guo J, Chen M, Yang S and Kung A H 2019 *Opt. Express* **27** 15638

[34] Huang H D, Teng H, Zhan M J, Xu S Y, Huang P, Zhu J F and Wei Z Y 2019 *Acta Phys. Sin.* **68** 070602 (in Chinese)